



Innovative laboratory unit for pre-testing of oxygen carriers for chemical-looping combustion

B. Fleiß¹ · J. Fuchs¹ · S. Penthor¹ · S. Arlt¹ · R. Pachler¹ · S. Müller¹ · H. Hofbauer¹

Received: 26 January 2021 / Revised: 16 April 2021 / Accepted: 19 April 2021
© The Author(s) 2021

Abstract

Chemical-looping combustion (CLC) is a highly efficient CO₂ separation technology with no direct contact between combustion air and fuel. A metal oxide is used as an oxygen carrier (OC) and acts in a dual fluidized bed as a separation tool and supplies the fuel with oxygen, which as an oxidation medium causes combustion to CO₂ and H₂O. The use of solid fuels, especially biomass, is the focus of current investigations. The OC plays a key role, because it must meet special requirements for solid fuels, which are different to gaseous fuels. The ash content, special reaction mechanisms, and increased abrasion make research into new types of OC essential. Preliminary testing of OC before their use in larger plants regarding their suitability is recommended. For this reason, this work shows the design and the results of a laboratory reactor, which was planned and built for fundamental investigation of OC. Designed as a transient fluidized bed, the reactor, equipped with its own fuel conveying system and an in situ solid sampling, is intended to be particularly suitable for cheap and rapid pre-testing of OC materials. During the tests, it was shown that the sampling device enables non-selective sampling. Different OC were tested under various operating conditions, and their ability to convert different fuels could be quantified. The results indicate that OC can be sufficiently investigated to recommend operation in larger plants.

Keywords Chemical-looping combustion · CLC · Oxygen carrier · OC · Pre-testing · Solid sampling

1 Introduction

Chemical-looping combustion (CLC) is considered a promising carbon capture technology [1]. The direct separation of CO₂ during combustion, by “inherent combustion,” does not require any further separation steps. This is achieved by using a so-called oxygen carrier (OC), which eliminates direct mixing of combustion air and fuel [2]. While CLC with gaseous fuels has already been demonstrated on a larger scale, biomass is seen as having particular potential as part of Bioenergy Carbon Capture and Storage (BECCS) and negative CO₂ emissions [3–5]. However, using solid fuels in CLC is more challenging compared to gaseous fuels, because of the inhomogeneous reactions, ash content, and the pollutant loading of the fuel. While on the one hand the reactor concept is

important, the selection of the OC also plays a key role in the development of the technology. A detailed investigation of different OC, especially natural ores or waste materials is essential for a better use of solid fuels with CLC [6]. Identification of suitable OC involves testing of samples at gram scale (e.g., in a thermogravimetric analysis, TGA) up to the several hundreds of kilogram in continuously operating pilot plants. Since testing should be fast and cost-effective (i.e., the use of personnel and consumables), initial screening of carriers in larger plants is not recommended. An intermediate step between small-scale facilities, such as TGA, and continuously operating units is necessary to bridge this gap. This work presents a lab-scale bubbling fluidized bed reactor, which can be operated alternately in reducing and oxidizing atmosphere to simulate the CLC operation. An innovative solid sampling device allows OC to be extracted from the reactor during operation. Its inventory and the gas volume flow can be varied, and thus, the reactor can meet the requirements of OC testing in terms of process conditions (e.g., temperature and gas velocities). Further, the batch operation allows for investigation of parameter variations, which cannot be realized in continuously operating units. Thus, the gap

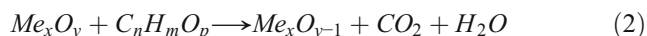
✉ B. Fleiß
Benjamin.Fleiss@tuwien.ac.at

¹ TU Wien, Institute of Chemical, Environmental and Bioscience Engineering (ICEBE), Getreidemarkt 9/166, 1060 Wien, Austria

between TGA and pilot reactor investigations of OC can be closed. The main goal is the cost-effective determination and selection of suitable OC for further use in dual fluidized beds of a larger scale. One step to achieve this is by commissioning, proof of concept, and validating the first experiments of the lab-scale unit presented in this work.

1.1 Chemical-looping combustion of solid biomass

CLC is a combustion technology that avoids a mixture of fuel and combustion air. To ensure this unmixed combustion, a metal oxide, the so-called oxygen carrier (OC), is used. The OC passes through two physically separated reaction zones to burn the fuel. In the first zone, an oxidation reaction (1), the OC binds oxygen during the reaction with air. Heat is released due to the exothermic reaction. The second reaction zone (2) is classified by a release of pure oxygen from the OC to the fuel. Combustion of the fuel takes place, and due to the absence of nitrogen, the product gas (ideally) consists solely of CO_2 and H_2O . This reaction step is also known as the reduction of the OC. After reduction, the OC returns to its “original” state before the first reaction step and the cycle starts again [7].



CLC distinguishes in its use between solid and gaseous fuels. Although the use of gaseous fuels is already well advanced, there is still much research work to be done for solid fuels [8]. These have recently become the focus of interest, as CLC of biomass could cause negative CO_2 emissions by application of CO_2 storage [3]. The aim is to reduce the CO_2 concentration in the atmosphere while at the same time producing electricity or heat. The challenge in using solid fuels is the ash content. The ash has to be separated from the OC, resulting in OC losses in addition to increased abrasion [9, 10]. Therefore, when solid fuels are used, natural ores or industrial waste materials are preferred in order to achieve better price and availability [5]. However, research is still being conducted to find the optimal OC, as the complicated interactions between OC, fuel, and ash cause unknown effects [6]. This increases the significance of identifying suitable OC for solid CLC.

Further, using solid biomass as fuel requires a thermochemical conversion of the fuel before the combustion. A reaction between fuel and OC does not take place directly, but gasification of the fuel via a gasification medium is necessary [11]. A suitable reactor model to implement this is the fluidized bed technology. Lewis and Gilliland (1954) designed a model of two connected fluidized beds, called a dual fluidized bed, which meets many of the requirements for CLC [12]. The two reaction steps of CLC are located in the different fluidized beds, and they are called air reactor (AR) and fuel reactor (FR), respectively, shown in Fig. 1.

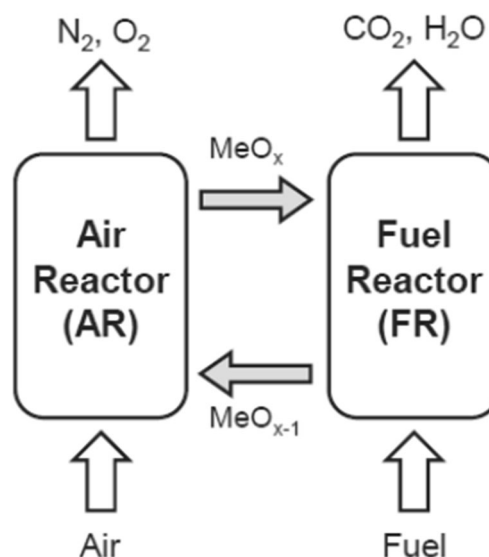


Fig. 1 Scheme of the CLC process with AR and FR [13]

2 Reactor concept

Previous pilot plants for solid CLC have been designed as a dual fluidized bed, like an 80 kW reactor constructed at TU Wien [14], a 100 kW reactor at Chalmers University of Technology [15], and a 1 MW_{th} pilot plant at Darmstadt University of Technology [16]. Further reactor concepts focus on a smaller scale, like an 1.5 kW_{th} demonstration reactor operated by the Spanish National Research Council [17]. In order to be able to investigate both the oxidation and the reduction reaction independently of each other, the reactor of this work is designed as a simple fluidized bed, i.e., alternating AR- and FR-operation can be simulated transiently.

The reactor has an inner diameter of 13 cm and a total height of about 1 m, whereby the fluidized bed is about 10 cm (see Fig. 2). About half of the height is a freeboard, which has been designed with a larger diameter to prevent particle discharge. Gas premixing takes place in a 10 cm high wind box. A nozzle bottom distributes the gas into the reactor and prevents bed material from trickling back into the wind box. A heating shell around the reactor should guarantee constant temperature conditions, but the special gas preheater, which can be operated with air as well as with steam, is also required.

A very important feature of the reactor is the in situ bed material sampling system, which allows the extraction of bed material through a moveable basket during hot operation. A motor can be controlled from the nearby digital interface, where parameters such as speed, sample duration, and penetration depth can be selected. Nitrogen flushing of the samples prevents contamination with ambient air. The frozen oxidation state of the material allows for a precise determination of the OC.

A further essential feature of the reactor is the possibility to use gaseous and solid fuels. Solid fuels are stored in a hopper located above the reactor. A screw conveyor doses the fuel,

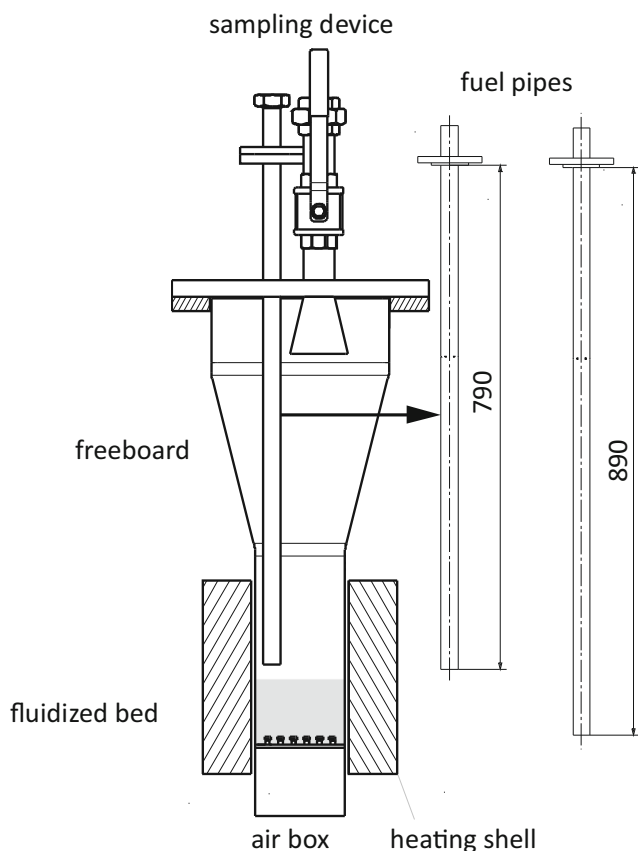


Fig. 2 Layout of the reactor with a sampling device, different fuel pipes, and heating shell

which falls through a pipe depending on the length onto or directly into the fluidized bed. Nitrogen flushing of the hopper prevents the formation of an igniting atmosphere and simultaneously acts as a carrier gas flow. Gaseous fuel can be introduced via the wind box below the bed. A picture of the laboratory unit can be seen in Fig. 3.

The measuring equipment of the reactor consists of temperature, pressure, and gas measurements to evaluate the experiments. The gas measurement corresponds to volume and concentration measurements of the five components CO_2 , CO , O_2 , H_2 , and CH_4 . Though a bypass, parts of the exhaust gas are transported via a condenser, then to a RME (rape methyl ester) scrubber and finally to the 5-component gas measurement device (see Fig. 4).

3 Material and methods

3.1 Fuels

Four different fuels are used in the experiments. These are biogenic fuels softwood, bark, and chicken manure in form of pellets with a length of about 6 mm. Furthermore, a fossil reference fuel was available: lignite with a crushed particle

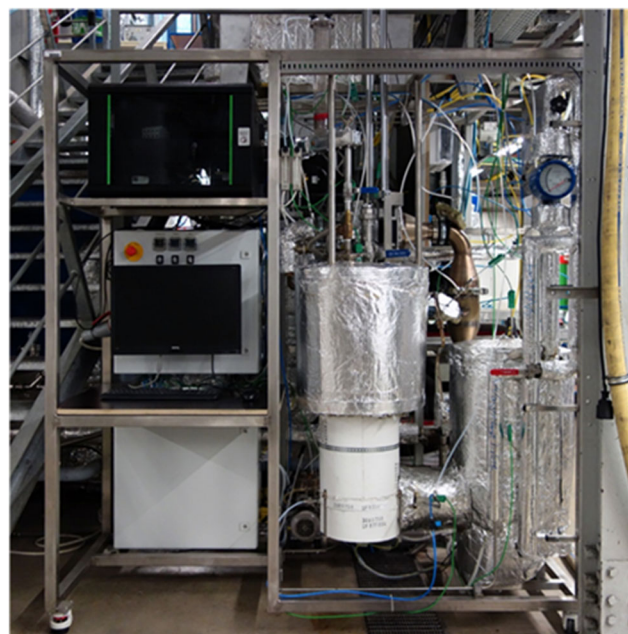


Fig. 3 Picture of the laboratory unit, on the left side the digital interface, in the middle of the fluidized bed, and on the right side of the gas preheater

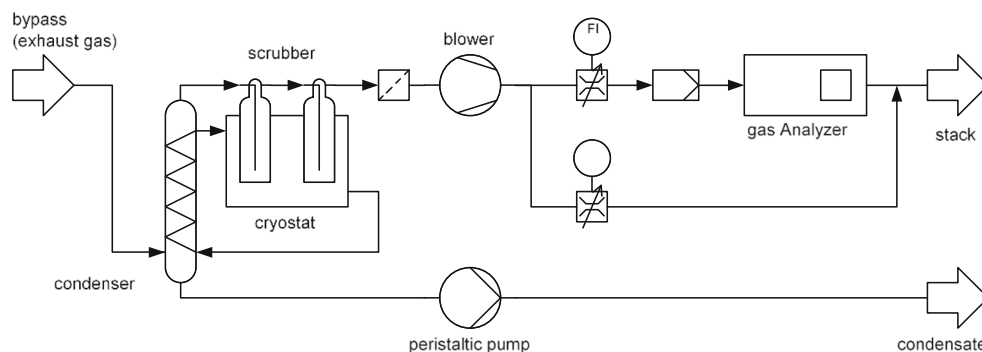
size of about 10 mm. The fuel analysis (ultimate and proximate) is shown in Table 1.

3.2 Oxygen carriers (OC)

Two different OC are tested and compared. Ilmenite, a titan-iron-oxide with great potential as OC [18], belongs to the OC with Het-CLC (heterogeneous) effect. Het-CLC OC cannot dispense gaseous oxygen or only in very small amounts [8]. Since the reaction takes place exclusively by gas-solid contact, gasification of the fuel is necessary to start the combustion reaction [19]. In contrast, the second material, braunite, a manganese ore, has properties of a Chemical Looping with Oxygen Uncoupling (CLOU) OC. A direct combustion reaction is possible, through a gaseous release of oxygen under the conditions prevailing in the fuel reactor [20]. The instability of the formed oxide triggers the partial release of the oxygen under certain conditions of temperature and oxygen partial pressure [21]. Since no gasification of the fuel is necessary, an inhomogeneous combustion reaction with much faster kinetics takes place. CLOU-OC tend to have higher fuel conversion rates, but so far, no natural ores with CLOU- O_2 levels comparable to synthetic OC have been identified [5, 19]. In addition, previously investigated natural ores with CLOU effect have been less promising regarding other important properties, such as long-term stability, mechanical resistance, and oxygen capacity [13].

Both OC, ilmenite and braunite, are dried for 24 h at 100 °C, and a thermal treatment at 600 °C is performed to prevent agglomeration of the particles. Table 2 shows the composition

Fig. 4 Configuration of the gas measuring section bypassing of the reactor exhaust gas stream



and important fluidized bed characteristics of the OC. For particle properties, sieve analyses, density, and bulk density measurements were carried out. A standard form factor ϕ of 0.8 was chosen, which is common for rounded sand. In addition, an element analysis by X-ray fluorescence spectroscopy was performed to investigate the OC composition of the OC.

3.3 Solid sampling device

With the novel constructed sampling device, it is possible to take samples directly from the fluidized bed while operating. The sampler is placed on the flange at the top of the reactor, as shown in Fig. 5. The sample basket is moved through a guiding tube into the reactor. When sampling, the sample tube and the connected basket are moved down into the reactor. When the basket reaches the lowest point, the position is held before moving back up. In the next step, a vacuum pump is started and the sampled bed material is transported from the basket into a sealable sample tube. Until the sample is sealed, it is constantly purged with N_2 during the sampling procedure to prevent atmosphere contamination. A detailed description can be found at Pachler (2019) [22].

Table 1 Composition of the used fuels

		Lignite	Softwood	Bark	Chicken manure
Water content	wt%	13.0	7.2	11.7	9.1
Ash	wt%(wf)	4.2	0.2	3.0	25.4
Carbon	wt%(wf)	65.5	50.7	55.7	38.0
Hydrogen	wt%(wf)	3.8	5.9	5.4	4.9
Oxygen	wt%(wf)	25.2	43.0	35.5	26.8
Nitrogen	wt%(wf)	0.8	0.2	0.4	4.1
Sulfur	wt%(wf)	0.4	0.0	0.0	0.3
Chlorine	wt%(wf)	0.1	0.0	0.0	0.5
Volatiles	wt%(waf)	51.8	85.4	69.9	67.7
LHV (dry)	kJ/kg(wf)	20800	18900	20300	13900

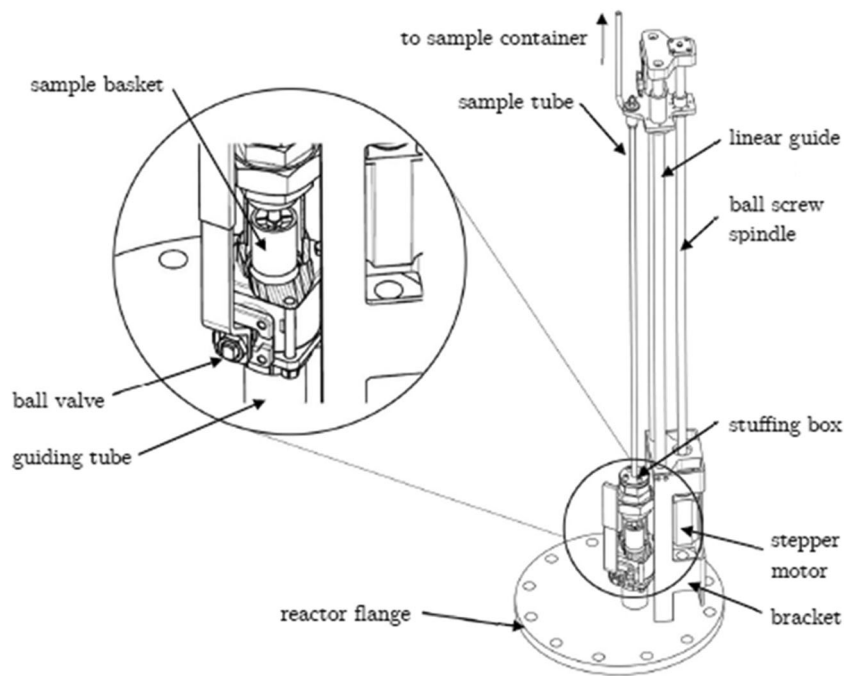
3.4 Experimental methods

One cycle of an experiment consists of an oxidation step and a reduction step. In the oxidation step, a $3 \text{ m}_{\text{STP}}^3/\text{h}$ air stream oxidizes the OC. Fig. 6 shows an increase of the component O_2 in the exhaust gas during the oxidation step “OX” until the concentration reaches the value of the ambient air. At this point, the OC is fully oxidized under the current process conditions and can no longer absorb any further O_2 . In the reduction step “RED”, steam replaces the air fluidization to ensure an oxygen-free atmosphere and cause the gasification of the fuel. As soon as the oxygen concentration drops to zero, the supply of a defined amount of fuel starts. This can be observed immediately by an increase of the gases CO_2 , CO , H_2 , and CH_4 . A CLC cycle is completed when these gases return to their original concentration, and to minimize errors and deviations, an experiment consists of five cycles.

Table 2 OC characteristics of ilmenite and braunite

Particle characteristics		Ilmenite	Braunite
d_p	μm	175	200
d_{sv}	μm	140	160
ϕ	-	0,8	0,8
ρ_p	kg/m^3	3820	3610
ρ_b	kg/m^3	2290	2170
OC composition			
Mn_3O_4	(wt%)	-	71.2
TiO_2	(wt%)	44.08	0.2
FeO	(wt%)	28.77	-
Fe_2O_3	(wt%)	17.66	14.3
SiO_2	(wt%)	1.99	7.6
MgO	(wt%)	3.58	0.3
Al_2O_3	(wt%)	0.64	4.4
MnO	(wt%)	0.3	-
CaO	(wt%)	0.32	1.3
S	(wt%)	0.14	0.04
Cr_2O_3	(wt%)	0.1	0.04

Fig. 5 Sampling device with sample basket to extract OC while operating [13]



An average cycle is calculated from the concentrations of the five cycles and is used for all further calculations. It is necessary to carry out at least five cycles, because the screw conveyor causes considerable fluctuations in the amount of fuel transported. If the last chamber of the screw conveyor is not emptied or completely emptied, the amount of fuel added varies from one cycle to the next. Nevertheless, the amount of fuel averaged over five cycles hardly deviates from the planned amount of fuel.

Nitrogen, higher hydrocarbons larger than C1, and tars are not measured. With the assumption that the flue gas contains only the five measured gases and nitrogen, Equation 3 can be

defined. This equation is based on the fact that the total volumetric flow is the sum of the individual volume flows, excluding higher hydrocarbons and tars. For the five components CO, CO₂, CH₄, H₂, and O₂, the measured concentrations φ_i can replace the volume flow.

$$\dot{V}_{\text{flue gas}} = \frac{\dot{V}_{N_2}}{1 - (\varphi_{CO} + \varphi_{CO_2} + \varphi_{CH_4} + \varphi_{H_2} + \varphi_{O_2})} \quad [\text{m}^3/\text{h}] \quad (3)$$

Although the total volume flow of flue gas is unknown, the nitrogen flow is not. The nitrogen volume comprises of the

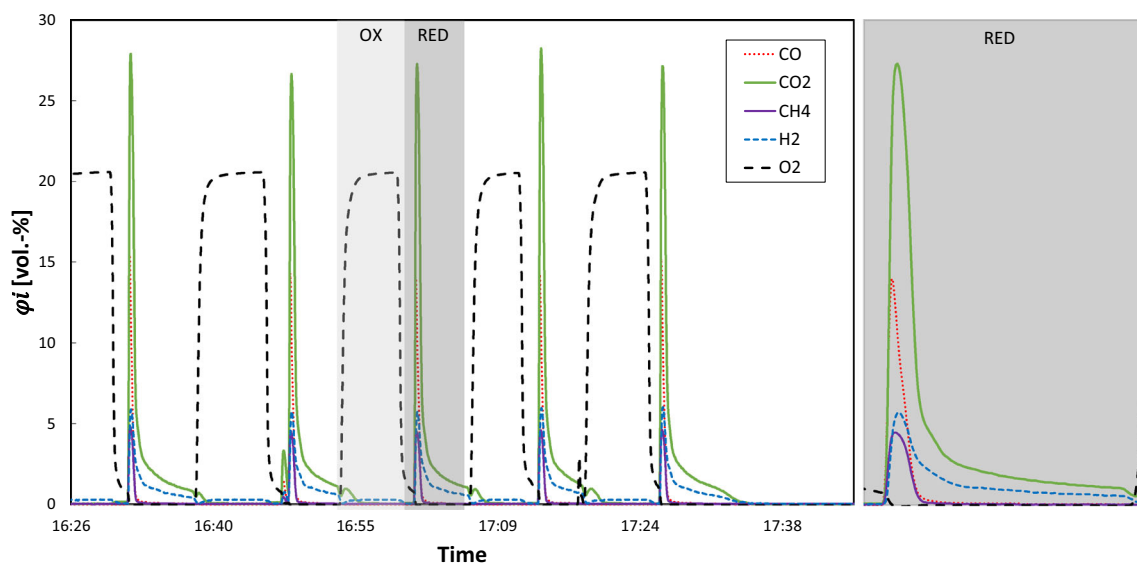


Fig. 6 Five experimental cycles illustrated by the five measured gas concentrations over time and a zoomed-in reduction cycle

flushing of screw conveyor and pressure sensors. Based on Equation 3, the total flue gas volume flow can be calculated. With the total volume flow and Equation 4, the volume flow of each single measured component can be determined.

$$V_i = V_{\text{flue gas}} \cdot \varphi_i \quad [\text{m}^3/\text{h}] \quad (4)$$

For further calculation, it is necessary to convert the volume flows to molar flows according to Equation 5. With regard to the general gas equation, the density ρ and molar mass M of the components are used to calculate the molar flows.

$$\dot{n}_i = \frac{\dot{V}_i \cdot \rho_i}{M_i} \quad [\text{mol/s}] \quad (5)$$

For each concentration measured, a molar flow value is obtained, with which the total moles can be calculated. These are more significant, because no continuous operation is processed. To obtain the total mole per component, the trapezoidal rule is used in Equation 6, in which t_k is the timestamp of the concentration measurement.

$$n_i = \sum_k (t_{k+1} - t_k) \cdot \frac{\dot{n}_i(t_k) + \dot{n}_i(t_{k+1})}{2} \quad [\text{mol}] \quad (6)$$

Consequently, important performance parameters can be assembled by calculating the total amount of the components. One of the key parameters is the carbon conversion rate X_C , which identifies and compares the reaction of fuel to gas [23]. Equation 7 shows the carbon conversion rate, calculated by dividing the amount carbon found in the gas phase by the carbon in the introduced fuel. The balance to 100% results from higher hydrocarbons, tars, and coke.

$$X_C = \frac{n_{C,\text{gas}}}{n_{C,\text{fuel}}} \cdot 100 \quad [\%] \quad (7)$$

Another important parameter is the CO_2 selectivity (S_{CO_2}). The selectivity is an indication of the complete fuel combustion. Thus, Equation 8 contains the amount of carbon in the exhaust gas $n_{C,\text{gas}}$ and the carbon contained in CO_2 (n_{CO_2}).

$$S_{\text{CO}_2} = \frac{n_{\text{CO}_2}}{n_{C,\text{gas}}} \cdot 100 \quad [\%] \quad (8)$$

A combination of the two previous performance parameters results in the CO_2 yield (Y_{CO_2}), Equation 9. It calculates the amount of carbon, converted to CO_2 , per fuel input of carbon.

$$Y_{\text{CO}_2} = X_C \cdot S_{\text{CO}_2} = \frac{n_{\text{CO}_2}}{n_{C,\text{fuel}}} \cdot 100 \quad [\%] \quad (9)$$

4 Results and discussion

4.1 Evaluation of the solid sampling device

Information about OC particles (e.g., oxidation state, morphology, and particle size distribution) and/or ash after oxidation and reduction steps is crucial for the evaluation of the performance of the OC and the process. Thus, it is important to verify that solid samples represent the whole bed material inventory and not only a certain particle size distribution. Therefore, the reactor was prepared with a known particle size distribution of ilmenite (see Fig. 7). The sampling tests have been performed under cold operating conditions, aiming at the almost identical area in the Grace diagram comparable to hot operation [24]. A sieve analysis of the sample taken provides information about the particle size distribution $q_3(d_{pi})$ and possible deviations. The input measurement is given in Fig. 7, on the left side, while the particle size distribution of the sample taken is shown on the right. In addition, the diagrams illustrate the corresponding cumulative distributions $Q_3(d_{pi})$ of the sieve analysis as a dashed line. The sieve diameter of both distributions, shown in Table 3, can also be calculated from the measurements. There is a deviation of only 0.5 percent, and this shows that the sampling is quite good and unselective. The deviation is in the range of the measurement accuracy. In this short fluidization time, no essential attrition can be expected and no other undesired effects (e.g., agglomeration) occurred.

Furthermore, it is important to validate the oxidation state of the solid samples in hot operation. The oxygen loading of an OC was evaluated over several cycles in the following experiment. The oxidation level of the OC can be determined by Equation 10 as the solid conversion of OC X_S [25].

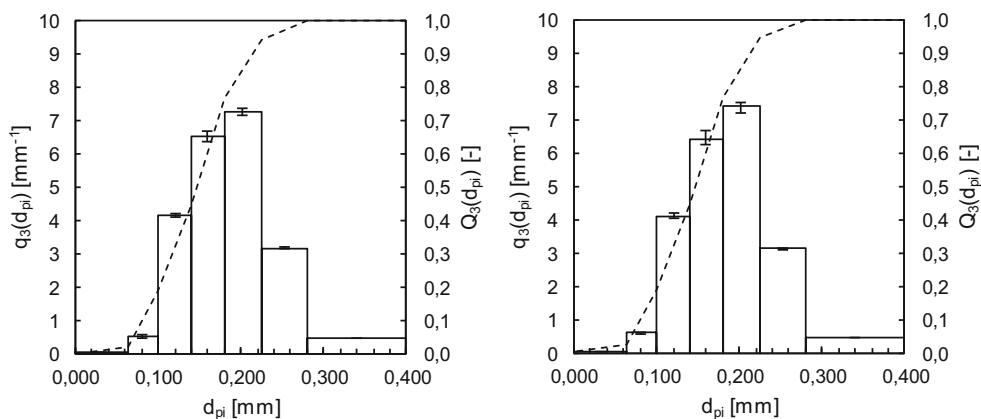
$$X_S = \frac{m - m_r}{m_o - m_r} \cdot 100 \quad [\%] \quad (10)$$

The variable m denotes the instantaneous mass of the OC, while m_r and m_o indicate the masses at full reduction and full oxidation. Kolbitsch et al. show a method determining these different masses of a sample [26]. With the verification of the solid sample device in cold operation, an experiment is proposed to test the OC while ongoing fuel supply at 950 °C. The aim of the experiment is to record X_S and thus the oxidation load of the OC to show that the sample of the sampling device

Table 3 Sauter diameter of sampling test

Sauter diameter	Initial	Sampling
d_p	173.9 μm	174.5 μm

Fig. 7 The particle size and the cumulative distribution of ilmenite. To the left, there is the result of the initial sample and on the right, the results extracted by the sampling device



accurately reflects the oxygen loading of the entire bed. For this purpose, the reactor is filled with 2.6 kg braunite and as fuel chicken manure is used.

After the OC is fully oxidized with air, fuel is gradually added. The fluidization takes place with 5 kg/h of steam, while 9.7 g of fuel per reaction cycle is introduced into the reactor. As there is no oxygen supply between the 13 cycles, the braunite should be reduced significantly. Five samples were taken, one in the fully oxidized state and further samples after the 1st, 3rd, 6th, and 13th cycle. For taking a solid sample in the reduction phase, flushing with nitrogen is necessary to dry the OC and freeze the oxidation state of the particle.

Figure 8 shows the measured oxidation level of the braunite samples. As expected, the measured X_S of the solid samples decreased continuously. After the 6th cycle, the OC releases only small amounts of oxygen, even though X_S only reaches around 60%. Reducing the braunite further requires higher temperatures or a different reduction medium than chicken manure. However, the oxidized sample (“Oxy”) does

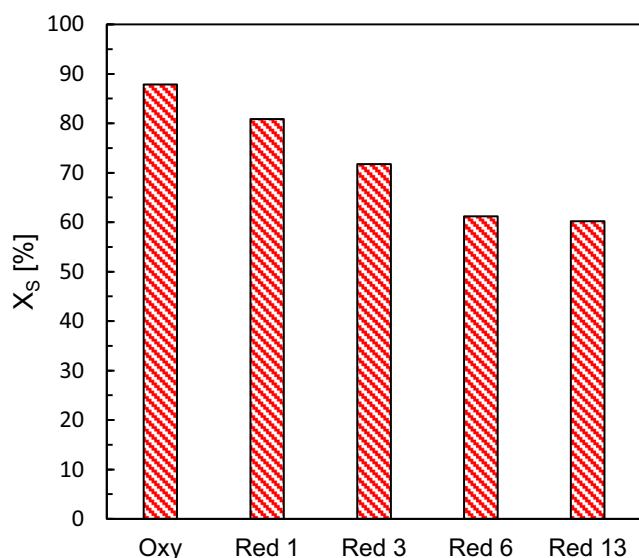


Fig. 8 Diagram of the solid conversion X_S of braunite while ongoing fuel supply

not reach the full oxidation state, which is defined by heating 24 h at 950 °C in an oven. A shorter residence time could be the reason for this. In this experiment, the reactor does not reach the full potential of the OC, but the sampling as well as the determination of the oxidation loading shows reliable results.

4.2 Operating conditions

The special reactor design enables the simulation of different experimental conditions. These include certain fluidization conditions in the bed, the reactor temperature, and an easy exchange of fuel and OC. This greatly simplifies the testing of the experimental conditions in different constellations. Starting from 950 °C and 5 kg/h steam fluidization, the operation conditions are varied to investigate their influence on the results. Different amounts of steam fluidization, bed temperatures, and a different OC are selected, as shown in Table 4. The table displays the carbon conversion rate and the CO₂ selectivity.

4.2.1 Fluidization

The reactor can be fluidized with either air, steam, or nitrogen. Experiments with 3.5 and 5 kg/h steam were carried out initially. When comparing the results of these two fluidization processes, an increase in both performance parameters with higher fluidization can be seen in Table 4. Higher fluidization means better mixing and thus increased gas-solid contact, which promotes the oxygen release. In addition, a higher steam-to-carbon ratio is known to increase the gasification rate of biomass [27]. In this case, the higher fluidization leads to an increase in carbon conversion and CO₂ selectivity of about 15 and 25%.

4.2.2 Temperature

Experiments with bed temperatures of 900 and 950 °C were carried out. With increasing temperatures, also the parameters,

Table 4 Results of the variation of steam fluidization, bed temperature, and oxygen carrier, including the carbon conversions rate X_C and the CO_2 selectivity S_{CO_2}

	Starting conditions	Change of parameter		
		Steam to 3.5 kg/h	Temperature to 900 °C	OC to ilmenite
X_C	87.4	71.3	81.8	79.7
S_{CO_2}	72.4	57.4	66.4	46.8

S_{CO_2} and X_C , rise. The sensibility of the system is shown, because minor changes of temperature cause noticeable effects. Higher temperatures not only have a positive impact on gasification kinetics but also improve the reactivity of the OC [6, 27]. Especially CLOU-OC like manganese ores show immense dependency on the temperature, because of falling stability of the oxide phase [20].

4.2.3 Oxygen carrier

The experiments also include ilmenite as OC. The reactor was filled with the same bulk height as utilized at the braunite experiments. All other process conditions remained unchanged. Ilmenite showed lower carbon conversion rates than braunite, whereby the low CO_2 selectivity was the biggest difference. The flue gas contains high amounts of CO and CH_4 , which indicates low oxygen delivery to the fuel. The reason for better performance of braunite can be traced back to the CLOU effect, which enables a faster release of oxygen [6, 20]. Especially the methane concentration is noticeably higher with ilmenite as OC. This effect has already been reported in literature [18]. In addition, the lower reactivity of ilmenite can be explained by a division of the iron phases into FeO and Fe_2O_3 . The FeO phase, which is more common in ilmenite, has higher temperature stability. This leads to the fact that the lattice oxygen of the ilmenite is released with greater difficulty at the given temperatures. Nevertheless, the Fe_2O_3 phase still has a higher standard heat of formation than other metal oxides, which also reflects the thermodynamic stability of the metal oxides [28]. This also indicates that braunite releases more lattice oxygen than ilmenite.

4.3 Influence of the geometry of fuel feeding

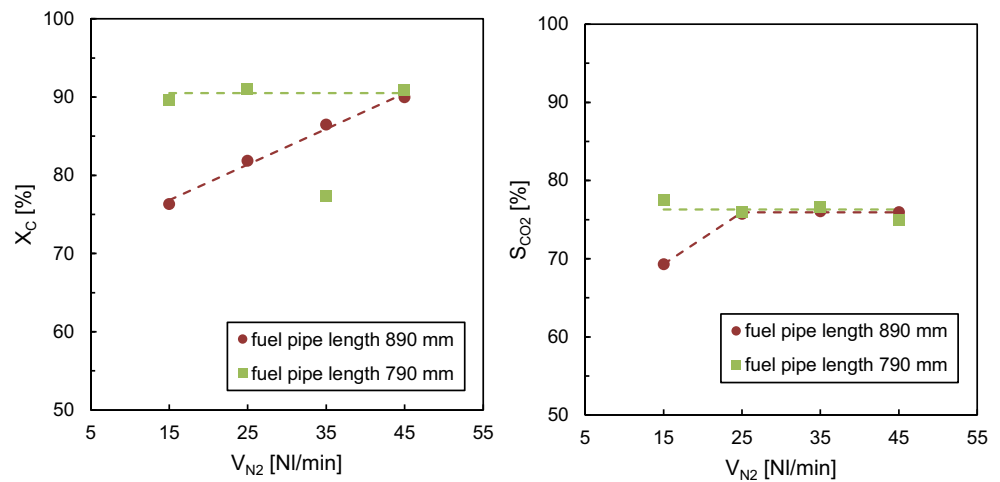
The fuel feeding system is of crucial importance in a fluidized bed system. It must ensure proper mixing to guarantee high heat transfer and intense contact with the steam and OC. The following experiments have the goal to optimize the fuel feeding system. Two fuel pipes of different lengths, 890 and 790 mm were used. The longer tube reaches directly into the bed of the fluidized bed and should immediately ensure good mixing between fuel and OC. However, the experiments do not confirm this assumption. For this reason, a comparison of two

experimental setups should provide additional information. For this purpose, braunite as OC, softwood pellets as fuel, and 5 kg/h steam fluidization were selected. The first experimental setup with the long fuel pipe involves an increase of the nitrogen flushing of the fuel transport system. The aim is by increasing the nitrogen flow rate from 15 to 25, 35, and 45 NI/min to increase the mixing of fuel and OC. For the second part of the experiment, the shorter fuel tube replaces the previous one, both shown in Fig. 2. The 790 mm long tube ends just above the fluidized bed surface. For the purpose of comparison, the nitrogen purging is also increased gradually. Fig. 9 shows the calculated performance parameters of the two experimental setups.

For the long fuel pipe, the fuel conversion rate increases with the volume flow of nitrogen. The CO_2 selectivity also increase from 15 to 25 NI/min nitrogen and then remained constant. Both performance parameters reach the level of the second experiment with higher flushing rates. The tests with the shorter pipe show hardly any deviation by applying different nitrogen purging and have consistently high performance. The only runaway value is the fuel conversion rate with 35 NI/min nitrogen. This experimental point was executed at a later stage. Although there was no further change to the operation conditions, than using fresh braunite, the high carbon conversion rates were not reached anymore. However, a possible activation of the OC over experimental time is not considered in these assumptions. The CO_2 selectivity still reached the same values compared to the other experiments.

In general, the outcome proves that the long fuel pipe has no positive effect on mixing or fuel conversion. Quite the contrary, a negative effect is indicated by the lower carbon conversion and CO_2 selectivity. One assumption that could be made is that floating of the pellets in the long fuel pipe occurs. Due to the low density of the pellets in contrast to the OC particles, the softwood pellets float in the pipe (see Fig. 10). This results in gasification of the fuel without sufficient oxygen supply for combustion. Only with a higher N_2 purge, the fuel is able to leave the fuel tube without restrictions and enables more contact between fuel and OC. In the case of the shorter fuel pipe, there are no restrictions and high performances are reached already with low purging rates of N_2 .

Fig. 9 Results of the variation of the fuel pipe length with rising nitrogen flushing flows. The carbon conversion rate on the left side and the CO₂ selectivity on the right



4.4 Influence of fuel type

After optimizing the fuel feeding system, the interaction of different fuels with an OC was investigated. The used biogenic fuels are softwood, bark, chicken manure, and lignite as a fossil reference fuel. The shape, size, and consistency of the fuels have a big influence on the feeding system. The wood pellets, for example, are characterized by high stability and resistance to fragmentation. This leads to a higher deviation of the amount of fuel transported to the reactor, because the screw conveyor has to crush some of the bigger pellets. The chicken manure and bark pellets, on the other hand, are softer and show less variation in fuel quantity. After leaving the screw conveyor, the chicken manure pellets have an extremely crumble consistency, which can improve the combustion reaction due to the increased surface area. The brittle structure of lignite is the only one of the four fuels that cause the formation of fine dust. Each fuel is examined at fluidizations with steam

of 3, 5, and 7 kg/h, at a temperature of 950 °C. Per cycle, the screw conveyor transports 9.7 g of fuel into the fluidized bed with a quantity of 2.6 kg of braunite. Figure 11 shows the results of the tests performed, represented by their CO₂ selectivity and yield of CO₂. The diagram shows that the fossil fuel achieves the highest CO₂ selectivity. The experiments with biogenic fuels result in 5–10% lower values in that order: bark, chicken manure, and softwood. This is consistent with the amount of volatiles in the fuels (see Table 1). Lower amounts of volatiles mean a better ratio to OC and CLOU-oxygen. The comparison of the CO₂ yields confirms that the performance of lignite has not been outstanding. Due to the low volatile content of coal, a higher proportion of coke was formed. For the other fuels, part of the larger quantity of volatiles was not fully converted. This resulted in high concentrations of CO and CH₄. Another influence factor was the structure of the fuels (Fig. 12), which can be analyzed by comparing bark and softwood. Both fuels have a similar fuel

Fig. 10 Floating of softwood pellets, comparison of the 890 mm and the 790 mm long fuel pipes

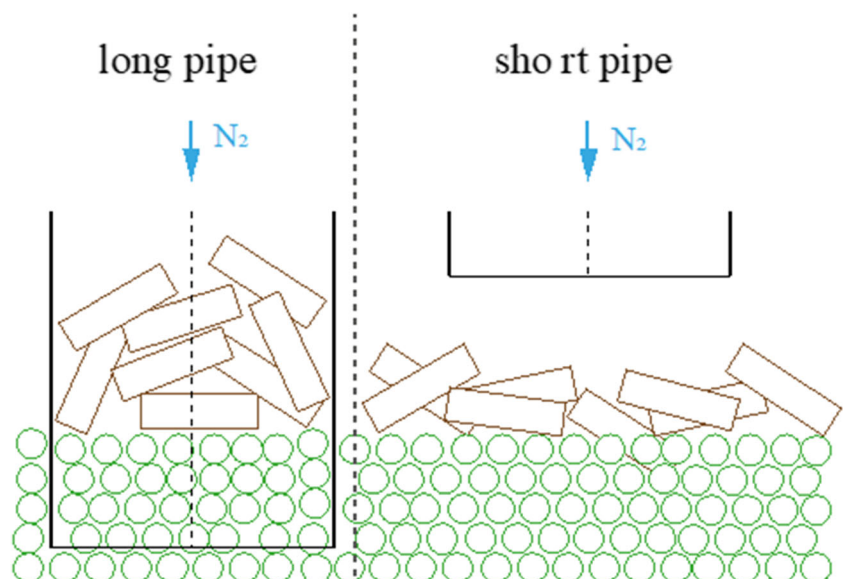
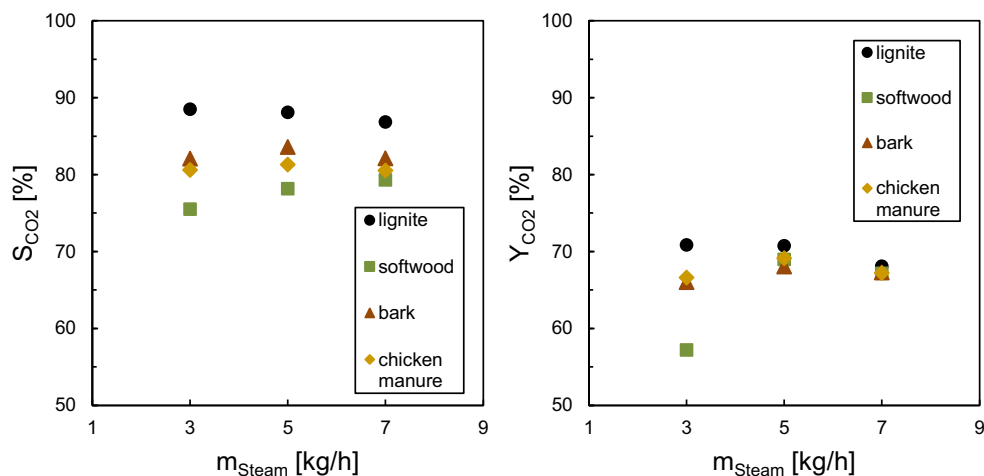


Fig. 11 The CO₂ selectivity and the CO₂ yield in an experiment with four different solid fuels, whereas lignite is a reference fossil fuel



composition, but the softer consistency of the bark pellets results in higher combustion rates. Interesting conclusions can be drawn by looking at the amount of steam. Softwood pellets show an increasing CO₂ selectivity and yield with the amount of steam. It can be assumed that gasification and decomposition of the stable structure of the softwood pellets occur faster with higher fluidization. Lignite, on the other hand, shows an opposite trend, possibly due to the discharge of fine coal dust with higher steam fluidization. Bark and chicken manure show hardly any variation over the increase in steam quantity.

5 Conclusion and outlook

In this study, a lab-scale reactor was tested regarding the investigation of OC used in the solid CLC technology. In more than 100 h of experimental time, the reactor has been extensively tested and the following conclusions could be drawn:

- It was proven that the reactor is equipped with a working sampling system, which can extract representative and nonselective samples during the experiments. Through the sampling system, the oxidation state and oxygen loading of the OC could be identified at any experimental point, representative for the entire filling of the reactor.
- A method was developed to calculate important parameters, namely, carbon conversion rate, CO₂ selectivity, and CO₂ yield, for assessing a transient experimental setup.
- The choice of OC has a significant impact on the performance of the CLC process. In this setup, with only brief contact between volatiles and OC, CLOU-OC are more suitable.
- The fuel feeding system could be improved by dropping the fuel on the fluidized bed instead of infusing it directly. This led to an improvement of fuel conversion and CO₂ selectivity.

Fig. 12 Investigated fuels from top-left to bottom-right: lignite, softwood, bark, and chicken manure



- Four different fuels were tested regarding their ability to be combusted using braunite as OC. Although the fossil lignite showed the highest numbers, biomass was not far away. The structure, consistence, and volatile content of the fuel could be identified as the most impactful properties besides interaction between fuel and OC.

In further work, a special focus should be laid on testing more different OC. The properties of the oxygen carriers should be investigated in more detail in order to be able to predict the operation in continuous larger plants. Thereby, a specific method of investigating the solid samples of the reactor should be developed as well. Particularly important will be the content of ash and coke residues in the solid sample as well as an exact and faster determination of the oxidation state and oxygen loading.

Acknowledgements The present work is part of the research projects BioLoop (872189) and OxyCar-FBC (857196) in cooperation with TU Graz: Institute of Chemical Engineering and Environmental Technology (CEET) and Institute for Thermal Engineering (ITE); National Institute of Chemistry: Department of Materials Chemistry; Spanish National Research Council: Department of Energy and Environment; Chalmers University of Technology; BEST GmbH; Rouge H2 Engineering GmbH; AVL List GmbH; Aichernig Engineering GmbH; Christof Project GmbH; SW-Energie Technik GmbH; TG Mess-, Steuer- und Regeltechnik GmbH; Rohkraft - Ing. Karl Pfehl GmbH; Göteborg Energi AB; Bertsch Energy GmbH & Co KG. It receives financial support from the research program “COMET” and “ERA-NET” by the Austrian Climate and Energy Fund.

Funding Open access funding provided by TU Wien (TUW). **Abbreviations** d_p , Sieve diameter [μm]; d_{sv} , Sauter diameter [μm]; M_i , Molar mass of the component i [g/mol]; m , Mass of OC [g]; m_o , Oxidized mass of OC [g]; m_r , Reduced mass of OC [g]; \dot{m}_{steam} , Mass flow of steam [kg/h]; $n_{C,\text{fuel}}$, Mol of carbon in the fuel [mol]; $n_{C,\text{gas}}$, Mol of carbon in the flue gas [mol]; n_{CO_2} , Mol of carbon of CO_2 in the flue gas [mol]; \dot{n}_i , Molar flow of the component i [mol/h]; n_b , Mol of the component i [mol]; $Q_3(d_{pv})$, Cumulative particle size distribution [-]; $q_3(d_{pv})$, Particle size distribution [mm^{-1}]; S_{CO_2} , CO_2 selectivity [%]; t_k , Timestamp [s]; $\dot{V}_{\text{flue gas}}$, Volume flow of the flue gas [m^3/h]; \dot{V}_i , Volume flow of the component i [m^3/h]; \dot{V}_{N_2} , Volume flow of nitrogen [Nl/min]; X_C , Carbon conversion rate [%]; X_S , Solid conversion [%]; Y_{CO_2} , CO_2 yield [%]; ϕ , Form factor [-]; ρ_p , Particle density [kg/m^3]; ρ_b , Bulk density [kg/m^3]; ρ_i , Density of the component i [kg/m^3]; φ_i , Volume fraction of the component i [-]; AR, Air reactor; BECCS, Bioenergy Carbon Capture and Storage; CLC, Chemical-looping combustion; CLOU, Chemical looping with oxygen uncoupling; $C_nH_mO_p$, Fuel; FR, Fuel reactor; HET-CLC, Heterogeneous chemical-looping combustion; LHV, Lower heating value; Me_xO_y , Metal oxide; OC, Oxygen carrier; OX/OXY, Oxidation step/cycle; RED, Reduction step/cycle; RME, Rape methyl ester; TGA, Thermogravimetric analysis

Open Access This article is licensed under a Creative Commons Attribution 4.0 International License, which permits use, sharing, adaptation, distribution and reproduction in any medium or format, as long as you give appropriate credit to the original author(s) and the source, provide a link to the Creative Commons licence, and indicate if changes were

made. The images or other third party material in this article are included in the article's Creative Commons licence, unless indicated otherwise in a credit line to the material. If material is not included in the article's Creative Commons licence and your intended use is not permitted by statutory regulation or exceeds the permitted use, you will need to obtain permission directly from the copyright holder. To view a copy of this licence, visit <http://creativecommons.org/licenses/by/4.0/>.

References

1. Solomon S, Qin D, Manning M (2007) Climate change 2007: the physical science basis. Contribution of Working Group I to the Fourth Assessment Report of the Intergovernmental Panel on Climate Change. IPCC 4
2. Agency IE (2010) Energy technology perspectives: scenarios & strategies to 2050. IEA. https://doi.org/10.1787/energy_tech-2010-en
3. Rydén M, Lyngfelt A, Langørgen Ø, Larring Y, Brink A, Teir S, Havåg H, Karmhagen P (2017) Negative CO_2 emissions with chemical-looping combustion of biomass – a Nordic energy research flagship project. Energy Procedia 114:6074–6082. <https://doi.org/10.1016/j.egypro.2017.03.1744>
4. Lindroos TJ, Rydén M, Langørgen Ø, Pursiheimo E, Pikkariainen T (2019) Robust decision making analysis of BECCS (bio-CLC) in a district heating and cooling grid. Sustainable Energy Technol Assess. 34:157–172. <https://doi.org/10.1016/j.seta.2019.05.005>
5. Adánez J, Abad A (2019) Chemical-looping combustion: Status and research needs. Proc Combust Inst 37(4):4303–4317. <https://doi.org/10.1016/j.proci.2018.09.002>
6. Adánez J, Abad A, Mendiara T, Gayán P, de Diego LF, García-Labiano F (2018) Chemical looping combustion of solid fuels. Prog Energy Combust Sci 65:6–66. <https://doi.org/10.1016/j.pecs.2017.07.005>
7. Pröll T (2011) Innovative fuel conversion with CO_2 capture using dual fluidized bed systems. Habilitation treatise, TU Wien
8. Lyngfelt A, Brink A, Langørgen Ø, Mattisson T, Rydén M, Linderholm C (2019) 11,000 h of chemical-looping combustion operation—where are we and where do we want to go? Int J Greenhouse Gas Control 88:38–56. <https://doi.org/10.1016/j.ijggc.2019.05.023>
9. Leion H, Mattisson T, Lyngfelt A (2008) Solid fuels in chemical-looping combustion. Int J Greenhouse Gas Control 2(2):180–193. [https://doi.org/10.1016/S1750-5836\(07\)00117-X](https://doi.org/10.1016/S1750-5836(07)00117-X)
10. Wang P, Howard B, Means N, Shekhawat D, Berry D (2019) Coal chemical-looping with oxygen uncoupling (CLOU) using a Cu-based oxygen carrier derived from natural minerals. Energies 12(8). <https://doi.org/10.3390/en12081453>
11. Abad A, Adánez J, Cuadrat A, García-Labiano F, Gayán P, de Diego LF (2011) Kinetics of redox reactions of ilmenite for chemical-looping combustion. Chem Eng Sci 66(4):689–702. <https://doi.org/10.1016/j.ces.2010.11.010>
12. Lyon RK, Cole JA (2000) Unmixed combustion: an alternative to fire. Combust Flame 121(1-2):249–261. [https://doi.org/10.1016/S0010-2180\(99\)00136-4](https://doi.org/10.1016/S0010-2180(99)00136-4)
13. Matzen M, Pinkerton J, Wang X, Demirel Y (2017) Use of natural ores as oxygen carriers in chemical looping combustion: a review. Int J Greenhouse Gas Control 65:1–14. <https://doi.org/10.1016/j.ijggc.2017.08.008>
14. Penthor SFJ, Benedikt F, Schmid J, Mauerhofer A, Mayer K, Hofbauer H (2018) First results from an 80 kW dual fluidized bed pilot unit for solid fuels at TU Wien. Paper presented at the 5th International Conference on Chemical Looping, Park City, Utah, USA

15. Markström P, Linderholm C, Lyngfelt A (2013) Chemical-looping combustion of solid fuels – design and operation of a 100 kW unit with bituminous coal. *Int J Greenhouse Gas Control* 15:150–162. <https://doi.org/10.1016/j.ijggc.2013.01.048>
16. Ohlemüller P, Ströhle J, Epple B (2017) Chemical looping combustion of hard coal and torrefied biomass in a 1 MW th pilot plant. *Int J Greenhouse Gas Control* 65:149–159. <https://doi.org/10.1016/j.ijggc.2017.08.013>
17. Abad A, Adánez-Rubio I, Gayán P, García-Labiano F, de Diego LF, Adánez J (2012) Demonstration of chemical-looping with oxygen uncoupling (CLOU) process in a 1.5kWth continuously operating unit using a Cu-based oxygen-carrier. *Int J Greenhouse Gas Control* 6:189–200. <https://doi.org/10.1016/j.ijggc.2011.10.016>
18. Cuadrat A, Abad A, Adánez J, de Diego LF, García-Labiano F, Gayán P (2012) Behavior of ilmenite as oxygen carrier in chemical-looping combustion. *Fuel Process Technol* 94(1):101–112. <https://doi.org/10.1016/j.fuproc.2011.10.020>
19. Mendiara T, Adánez-Rubio I, Gayán P, Abad A, de Diego LF, García-Labiano F, Adánez J (2016) Process comparison for biomass combustion: in situ gasification-chemical looping combustion (iG-CLC) versus chemical looping with oxygen uncoupling (CLOU). *Energy Technol* 4(10):1130–1136. <https://doi.org/10.1002/ente.201500458>
20. Mattisson T, Lyngfelt A, Leion H (2009) Chemical-looping with oxygen uncoupling for combustion of solid fuels. *Int J Greenhouse Gas Control* 3(1):11–19. <https://doi.org/10.1016/j.ijggc.2008.06.002>
21. Mayer K, Piesenberger S, Penthor S, Pröll T, Hofbauer H (2018) Chemical looping combustion using two different perovskite based oxygen carriers: a pilot study. *Energy Technol* 6:2333–2343. <https://doi.org/10.1002/ente.201800244>
22. Pachler R (2019) Chemical looping combustion – a sustainable combustion technology for negative emission energy production. Doctor thesis, TU Vienna, Vienna
23. Mei D, Zhao H, Ma Z, Zheng C (2013) Using the sol-gel-derived CuO/CuAl₂O₄ oxygen carrier in chemical looping with oxygen uncoupling for three typical coals. *Energy Fuel* 27(5):2723–2731. <https://doi.org/10.1021/ef3021602>
24. Grace JAA, Knowlton T (1997) *Circulatin fluidized beds*. Balckie Academic and Professional, 1st edn. Springer, Netherlands. <https://doi.org/10.1007/978-94-009-0095-0>
25. Adanez J, Abad A, Garcia-Labiano F, Gayan P, de Diego LF (2012) progress in chemical-looping combustion and reforming technologies. *Prog Energy Combust Sci* 38(2):215–282. <https://doi.org/10.1016/j.pecs.2011.09.001>
26. Kolbitsch P, Pröll T, Bolhar-Nordenkamp J, Hofbauer H (2009) Characterization of chemical looping pilot plant performance via experimental determination of solids conversion. *Energy Fuel* 23(3):1450–1455. <https://doi.org/10.1021/ef8008184>
27. Schmid JC, Benedikt F, Fuchs J, Mauerhofer AM, Müller S, Hofbauer H (2019) Syngas for biorefineries from thermochemical gasification of lignocellulosic fuels and residues—5 years’ experience with an advanced dual fluidized bed gasifier design. *Biomass Convers Biorefin*. <https://doi.org/10.1007/s13399-019-00486-2>
28. Alalwan HA, Augustine LJ, Hudson BG, Abeysinghe JP, Gillan EG, Mason SE, Grassian VH, Cwiertny DM (2021) Linking solid-state reduction mechanisms to size-dependent reactivity of metal oxide oxygen carriers for chemical looping combustion. *ACS Appl Energy Mater* 2021 4(2):1163–1172. <https://doi.org/10.1021/acsaem.0c02029>

Publisher’s Note Springer Nature remains neutral with regard to jurisdictional claims in published maps and institutional affiliations.